Thermochimica Acta 612 (2015) 34–39

Contents lists available at ScienceDirect

Thermochimica Acta

journal homepage: www.elsevier.com/locate/tca

Polymorphism of lead oxoborate

A.G. Tyulyupa [a], V.V. Voronov [b], P.P. Fedorov [b,*]

[a] Middle School, Sablinskoe, Stavropol region, 356322, Russia
[b] A.M. Prokhorov General Physics Institute RAS, 38 Vavilov Street, Moscow 119991, Russia

ARTICLE INFO

Article history:
Received 16 October 2014
Received in revised form 8 May 2015
Accepted 12 May 2015
Available online 14 May 2015

Keywords:
Lead borate
Undercooling
Allotropy
Polymorphism
Nonlinear crystal
Metastable phase transition
Differential thermal analysis

ABSTRACT

The study of lead borate melt crystallization by differential thermal analysis (DTA) and X-ray diffraction analysis has shown that, for $Pb_4O(BO_3)_2$ (or $4PbO{\cdot}B_2O_3$) stoichiometric compound, its well-known orthorhombic modification (non-centrosymmetric *Aba*2 space symmetry group (SSG), $a = 15.472(1)$, $b = 10.802(1)$, $c = 9.9486(6)$ Å unit cell parameters) is metastable. It forms from the undercooled melt and has a melting point of 530 ± 5 °C.

1. Introduction

Lattices of the single crystals of various composition borates are formed in non-centrosymmetric space symmetry groups. This phenomenon is linked to the complexity of anionic fragments in crystalline borates. As a result, they possess certain unique physical features, including non-linear optical (NLO) properties. Such non-linear crystals are capable of efficient transformation of laser irradiation and, therefore, can be used in high-power monochromatic sources of ultra-violet (UV) irradiation. In addition to their unique optical properties (wide spectrum region of optical transparency that reaches 150–200 nm boundary in the UV part of the spectrum [1,2]), borates, generally, have excellent mechanical properties and high optical damage thresholds that give them serious advantages over other oxygen-containing optical crystals such as phosphates, niobates, titanates, molybdates, iodates, nitrites, etc.

The class of borate optical materials includes a couple of widely used compounds: β-BaB_2O_4 (BBO) [3–5], LiB_3O_5 (LBO) [6], as well as some other materials such as: CsB_3O_5 (CBO) [7], $LiCsB_2O_8$ (CLBO) (YCOB) [19], $BaAlBO_3F_2$ (BABF) [20], $La_2CaB_{10}O_{19}$ (LCB) [21], $Y_{0.57}La_{0.72}Sc_{2.71}(BO_3)_4$ (YLSB) [22,23], etc. Along with quantum chemistry calculations and crystallography investigations [1,2,24], studying phase equilibria in the above oxide and fluoride systems are crucial for development of the single crystal growth technology and obtaining borate single crystals of the required size and high optical quality as it has been unequivocally demonstrated for LBO [25], BBO [26–30], and KBBF [1,10].

Recently, when a novel $Pb_4O(BO_3)_2$ NLO borate was discovered, it was found as expected that its space symmetry group (SSG) *Aba*2 lacks a center of inversion [31,32]. $Pb_4O(BO_3)_2$ crystalline samples were prepared by quickly controlled quenching of the melt to 470 °C (the starting material was preliminarily prepared by melting a mixture of PBO and H_3BO_3, gradually heating to 600 °C, and seasoning at this temperature for 20 h). In fact, the aforementioned $Pb_4O(BO_3)_2$ compound was described much earlier by Geller and Bunting [33] as $4PbO{\cdot}B_2O_3$ in the course of their study of the $PbO–B_2O_3$ system phase diagram. This compound undergoes a phase transformation at 552 °C and melts congruently at 565 °C. Existence of $4PbO{\cdot}B_2O_3$ was also independently confirmed in [34] while studying phase equilibria in the $PbO–B_2O_3–WO_3$ ternary system. In addition, McMurdie [35] published an unindexed X-ray diffraction pattern of $Pb_4O(BO_3)_2$, but his data do not agree with the similar results in [31,32]. The reason why scientists did not pay enough attention to $Pb_4O(BO_3)_2$ stems from the fact that the growth of $Pb_4O(BO_3)_2$ single crystals has been seriously hindered by the polymorphous phase transition of this compound despite the congruent character of the melting.

* Corresponding author. Tel.: +7 499 503 8292.
E-mail addresses: ppfedorov@yandex.ru, ppf@lst.gpi.ru (P.P. Fedorov).

http://dx.doi.org/10.1016/j.tca.2015.05.010
0040-6031/

Therefore, the purpose of our study was to further investigate the phase formation during crystallization of the $Pb_4O(BO_3)_2$ composition melt, $Pb_4O(BO_3)_2$ polymorphous phase transformation, and determine the conditions for the synthesis of $Pb_4O(BO_3)_2$ polymorph with non-linear optical properties.

2. Experimental

We used commercially available 99.5 wt.% pure lead oxide PbO (TU 6-09-5382-88 standard) and 99.9 wt.% pure boron oxide B_2O_3 (TU 6-09-3558-78 standard) from the Red Chemist manufacturer (St. Petersburg, Russia) as our starting materials. Prior to DTA experiments, PbO and B_2O_3 specimens were heated at 300–400 °C for 2 h to remove traces of moisture. Samples were weighed with MASSA-K electronic balance (0.005 g accuracy for 1 g samples).

X-Ray diffraction phase analysis (Brucker D8 Discover diffractometer, CuKα radiation, Ni filter) data for the polycrystalline $Pb_4O(BO_3)_2$ powder samples were treated with the use of TOPAS software package.

We investigated $Pb_4O(BO_3)_2$ phase transitions under heating and cooling conditions with the use of a differential thermal analysis (DTA) technique and our own proprietary DTA installation under air. Studied specimens (0.6–0.8 g) were placed in platinum crucible (1 ml). Alumina powder (1 g) was used as a standard reference material. Nichrome coiled wire served as a heating element. Grog alumina clay (shamotte) was utilized for thermal insulation, and zirconia ceramic pieces served as cover lids for the heating chamber sides. The cold junctions of the thermocouples were kept in ice–water at 0 °C. Temperature in the oven heating zone was regulated by the TRM-151 regulator (programmed controller manufactured by OVEN, Moscow, Russia). Signals from chromel–alumel (type K) thermocouples were registered by ZET-220 unit (ETMS, Moscow/Zelenograd, Russia) and treated with the use of ZetLab computer software. In order to enhance our DTA installation sensitivity to undercooling processes, we registered signal from the thermocouple attached to the crucible with the studied sample (instead of the reference sample) during thermal analysis experiments (i.e., temperature difference (DTA) vs. temperature (TA) curves, respectively). Thermocouples were calibrated in respect to NaCl (99.99 wt.% pure) melting point, and Na_2SO_4 (99.5 wt.% pure) melting point and polymorphic transition temperature. We evaluate the accuracy of temperature determination in our experiments as ±5 °C.

DTA curves were recorded for heating and cooling experiments at 5 °C/min for both types of experiments.

PbO was placed in a platinum crucible, then it was melted, and small portions of B_2O_3 were added later until $Pb_4O(BO_3)_2$ ($4PbO{\cdot}B_2O_3$) stoichiometry was achieved. Finally, the sample temperature was raised up to 950 °C to make the specimen homogeneous. Mass losses during such procedure did not exceed 1%.

3. Results and discussion

Both heating and cooling DTA curves (Fig. 1, curves 1 and 2, respectively) for $Pb_4O(BO_3)_2$ samples were complex and contain two thermal effects. Temperatures of such effect maxima in the cooling curve differed from ones in the heating curve by 12–14 °C or less (Fig. 1); but, nevertheless, the starting points of effects (552 °C for $\beta \rightarrow \alpha$ phase transition and 565 °C for $\alpha \rightarrow$ liquid transformation) were in a good agreement with the corresponding data [33] for the B_2O_3–PbO system.

However, crystallization of $Pb_4O(BO_3)_2$ usually occurred from an undercooled melt (Fig. 1, curves 3). The temperature increase after the beginning of crystallization unequivocally indicated an exothermal character of the latter process as well as metastability of the undercooled liquid phase. Temperatures of crystallization from such undercooled melts at the same 5 °C/min cooling rate varied over a fairly broad interval (up to 100 °C). This confirmed the random crystallization nucleation mechanism in the melt [36,37]. Such random undercooling is quite typical in the case of poor wetting ability of the melt with the crucible [38].

Multiple heating experiments with $Pb_4O(BO_3)_2$ ($4PbO{\cdot}B_2O_3$) samples have shown that melting occurred at different temperatures. Corresponding DTA curves of such experiments could be arranged into two groups (Fig. 2): those that could be characterized as stable (S) or metastable (M) systems. The difference between $Pb_4O(BO_3)_2$ melting points in the S- and M-type curves was about 30 °C. S-Type DTA curves corresponded to the β-$Pb_4O(BO_3)_2 \rightarrow \alpha$-$Pb_4O(BO_3)_2$ phase transformation and melting of α-$Pb_4O(BO_3)_2$ phase [33]. M-Type curves, apparently, corresponded to the $Pb_4O(BO_3)_2$ samples with a different crystalline structure (let us refer to it as the γ-$Pb_4O(BO_3)_2$ phase).

Multiple heating/cooling DTA experiments with such metastable γ-$Pb_4O(BO_3)_2$ specimens produced typical thermograms depicted in Fig. 3. Similar to α-$Pb_4O(BO_3)_2$, γ-$Pb_4O(BO_3)_2$ melts

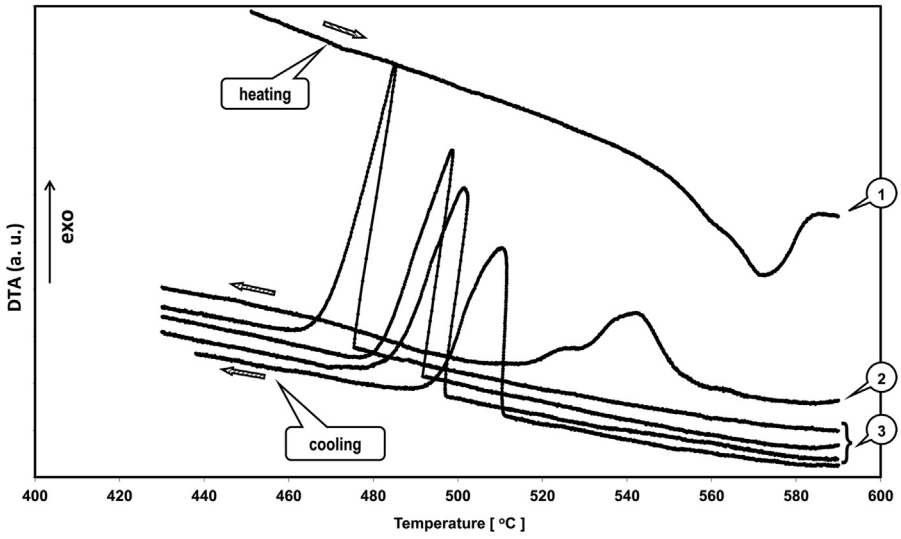

Fig. 1. Typical $Pb_4O(BO_3)_2$ DTA curves (5 °C/min): heating (1), cooling with crystallization without undercooling (2), and cooling with undercooling crystallization (3).

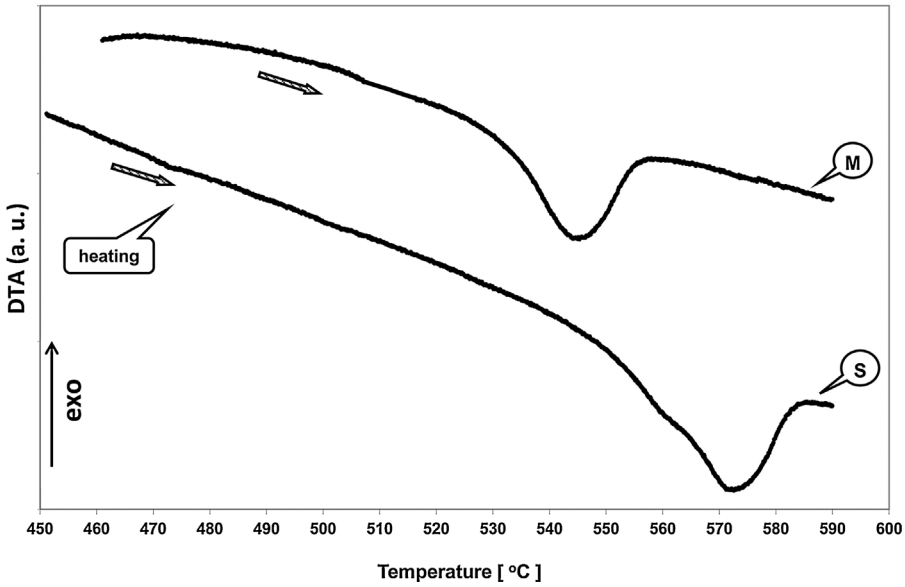

Fig. 2. Typical $Pb_4O(BO_3)_2$ heating (melting) DTA curves for the stable (S) and metastable (M) specimens (α-$Pb_4O(BO_3)_2$ and γ-$Pb_4O(BO_3)_2$ phases, respectively).

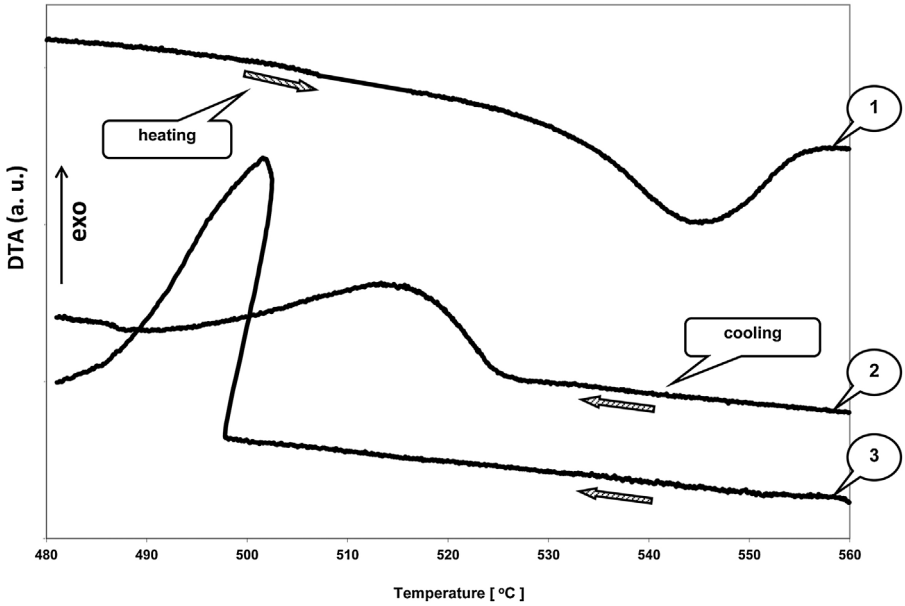

Fig. 3. Typical γ-$Pb_4O(BO_3)_2$ DTA curves: heating (1), cooling without undercooling crystallization (2), and cooling with undercooling crystallization (3).

were also prone to serious undercooling. However, γ-$Pb_4O(BO_3)_2$ heating and cooling curves (Fig 3, curves 1 and 2, respectively) contained only one peak vs. the two-peaked β-$Pb_4O(BO_3)_2$ DTA curves (Figs. 1–3).

These observations resulted in our further studying the factors affecting how $Pb_4O(BO_3)_2$ actually melted and crystallized (Fig. 4). Namely, we carried out repeated heating and cooling experiments while varying the temperature to which γ-$Pb_4O(BO_3)_2$ samples were cooled down before the next heating cycle was initiated (Fig. 4). As a result, our DTA experiments, performed with $Pb_4O(BO_3)_2$ samples that were repeatedly heated/cooled to the various temperatures (Fig. 4), have shown that:

- samples with $Pb_4O(BO_3)_2$ stoichiometry melted at different temperatures, depending on their phase composition. These temperatures could vary by up to 30 °C;

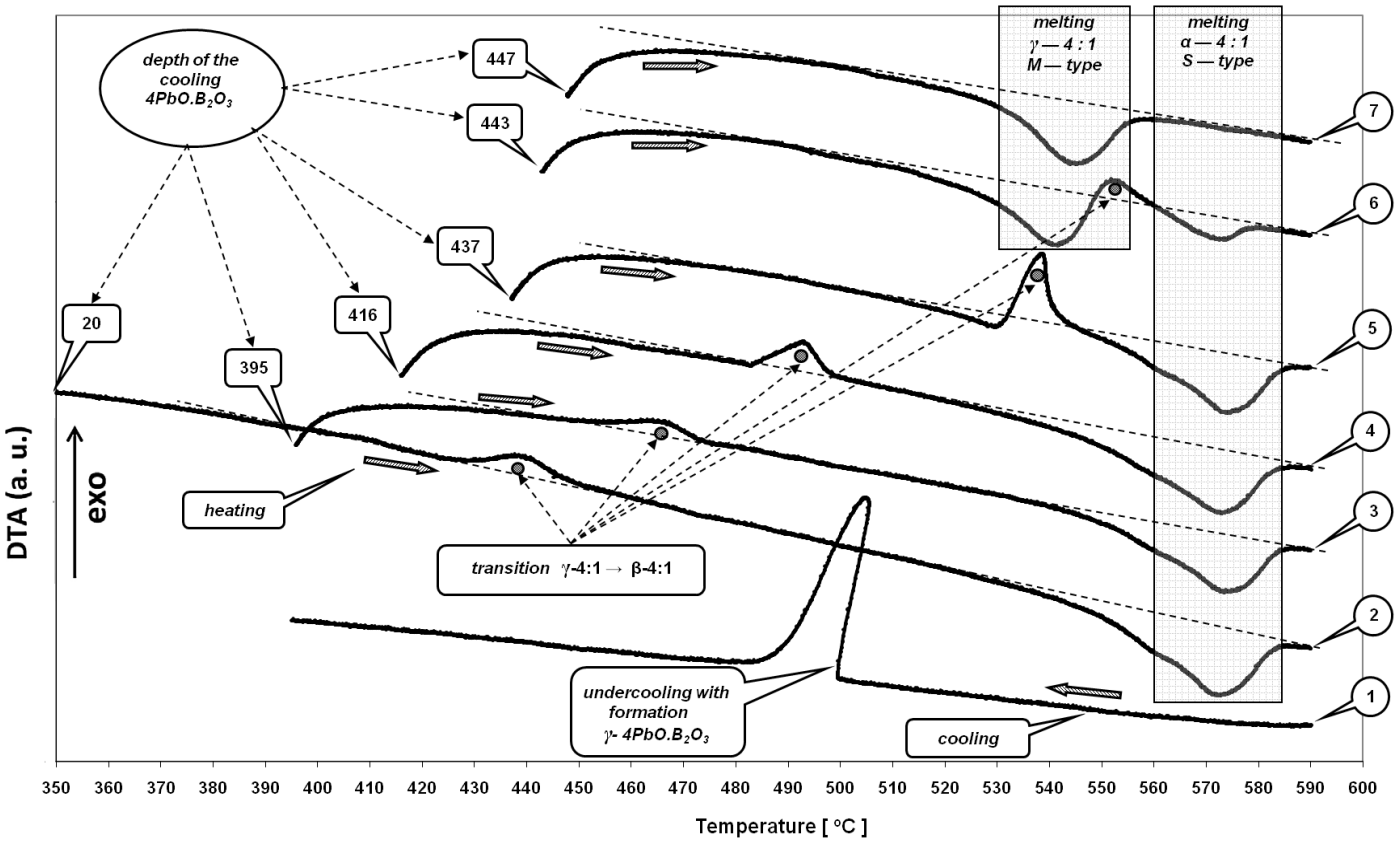

Fig. 4. Typical γ-$Pb_4O(BO_3)_2$ DTA curves: cooling with overcooling crystallization (1), heating with various temperature preliminary cooling (2–7).

- the type of $Pb_4O(BO_3)_2$ melting (i.e., S- or M-type) was determined by thermal prehistory of the specimen, i.e., how deeply the sample has been precooled before the subsequent heating: if $Pb_4O(BO_3)_2$ was cooled below 440 °C, it melted as an S-type (thermograms 2–5, Fig. 4), but if it was cooled to the temperature above 445 °C, it melts as an M-type (curve 7, Fig. 4);
- if the $Pb_4O(BO_3)_2$ sample has been cooled below 440 °C, then its DTA heating curves had an exothermic effect, but the position (temperature) of such exothermic effect depended on how deeply the specimen had been cooled (curves 2–6 in Fig. 4);
- in the experiments, when the location of the above "migrating" exothermic effect coincided with the M-type $Pb_4O(BO_3)_2$ melting temperature, the whole sample did not melt completely at the same temperature; the rest of the sample has finished melting as per the S-type (curve 6, Fig. 4).

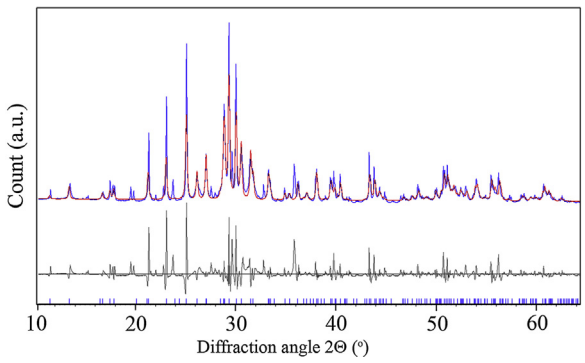

Fig. 5. X-ray diffraction pattern of γ-$Pb_4O(BO_3)_2$ phase (sample no. 1) in comparison to [38] data: experimental and theoretical curve produced by TOPAS software for *Aba*2 space symmetry group (SSG) and $a = 15.472(1)$, $b = 10.802(1)$, $c = 9.9486(6)$ Å unit cell parameters (1); differential curve (2); position of the lines at the theoretical curve (3).

The crystallization of the sample which was cooled to 443 °C (thermogram 6, Fig. 4) is of special interest. This sample was a quenched γ-$Pb_4O(BO_3)_2$ phase, but started melting according to the M-type transformation. Nevertheless, further heating resulted in an exothermic effect corresponding to transformation of unmelted part of the sample to an equilibrium phase followed by S-type melting. Perhaps, this effect was caused by the size of the relatively large sample utilized in our studies.

Typical X-ray diffraction data for M-melting γ-$Pb_4O(BO_3)_2$ samples are presented in Fig. 5 (sample No. 1 was prepared from the melt cooled from 750 °C to the ambient temperature at 10 °C/min cooling rate). Sample No. 1 contains more than 95% of the orthorhombic phase with $a = 15.472(1)$, $b = 10.802(1)$, $c = 9.9486(6)$ Å unit cell parameters, which is close to the previously obtained data [31].

Our experimental data can be explained with the use of chemical thermodynamic potentials for various $Pb_4O(BO_3)_2$ ($4PbO{\cdot}B_2O_3$) phases schematically depicted in Fig. 6. All shown $G(T)$ curves are convex and decreasing. There are three polymorphous modifications in the system: high temperature α-$Pb_4O(BO_3)_2$, low temperature β-$Pb_4O(BO_3)_2$, and metastable γ-$Pb_4O(BO_3)_2$. Also there are four phase transformation temperatures: $T_1 = 552$ °C (β ↔ α polymorphous transformation), $T_2 = 565$ °C (α ↔ L melting of the high-temperature polymorphous modification), unknown T_3 (β ↔ L metastable melting of the low-temperature modification), and $T_4 = 530$ °C (γ ↔ L metastable melting of the non-equilibrated modification). Fedorov and Sobolev [39] showed that the temperature of metastable melting

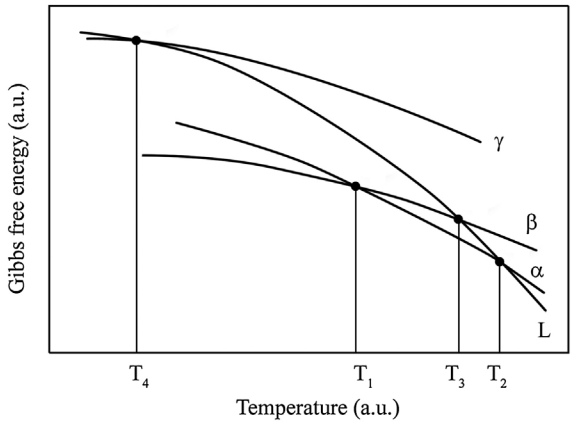

Fig. 6. Temperature dependencies of isobaric–isothermal potentials of 3 competing lead borate phases (α-, β-, and γ-) and the melt (L) of $Pb_4O(BO_3)_2$ compound (schematic depiction).

(T_3) of the low temperature modification, when the G(T) curves for the melt and the low-temperature β-modification intersect each other, can be calculated by the following equation:

$$T_3 = \frac{(T_1\Delta S_1 + T_2\Delta S_2)}{(\Delta S_1 + \Delta S_2)},$$

where ΔS_1 and ΔS_2 are the entropies of the $\beta \leftrightarrow \alpha$ polymorphous transition and $\alpha \leftrightarrow$ L melting, respectively.

In view of the above said, we have redrawn a part of the PbO–B_2O_3 phase diagram [33] (Supplemental material, Fig. 3), considering metastable γ-$Pb_4O(BO_3)_2$ phase equilibria. Please note that if the melt is undercooled to some phase metastable melting point, then such metastable phase crystals should form from the said melt in accordance with Ostwald's step rule (e.g., see [40,41] for this phenomenon in the similar case of undercooled rare earth fluoride melts).

In conclusion, our data unequivocally indicate that in order to obtain γ-$Pb_4O(BO_3)_2$ non-linear single crystals directly from the melt of the same chemical composition, one has to overcool such melt down to the temperature of its metastable melting, i.e., 530 °C. This is a mandatory condition, and the latter is in complete agreement with previously published data [31] regarding the preparation of $Pb_4O(BO_3)_2$ non-linear optical phase.

Also it is worth mentioning that the metastable phases, similar to those discussed above, are quite common for borate systems because of the high viscosity of borate melts, which, in turn, is caused by the presence of complex boron–oxygen radicals (fragments) in these melts: thus, the Na_2O–B_2O_3 system [42] has been a very bright example of the complex polymorphism; and formation of metastable phases was observed for PbB_2O_4 [43] as well.

4. Conclusion

Our data confirm that the non-linear optical phase of $Pb_4O(BO_3)_2$, described earlier in [31,32], is a metastable γ-$Pb_4O(BO_3)_2$ modification. Its single crystals can be grown from melts undercooled below 530 °C.

Acknowledgments

We are grateful to A.I. Popov, R. Simoneaux and E.V. Chernova for their assistance with preparing this manuscript.

Appendix A. Supplementary data

Supplementary data associated with this article can be found, in the online version, at http://dx.doi.org/10.1016/j.tca.2015.05.010.

References

[1] Chuangtian Chen, Takatomo Sasaki, Rukang Li, et al., Nonlinear Optical Borate Crystals, Wiley-VCH, Weinheim, 2012.
[2] V. Pasiskevicius, Nonlinear crystals for solid-state lasers, in: B. Denker, E. Shlovsky (Eds.), et al., Handbook of Solid-State Lasers, Woodhead Publishing, Oxford, 2013 pp. 139–167.
[3] C.T. Chen, B.C. Wu, A.D. Jiang, G.M. You, A new type ultraviolet SHG crystal: β-BaB_2O_4, Sci. Sin. B 28 (1985) 235–241.
[4] P.P. Fedorov, A.E. Kokh, N.G. Kononova, Barium borate β-BaB_2O_4 as a material for nonlinear optics, Russ. Chem. Rev. 71 (2002) 651–671.
[5] T.B. Bekker, A.E. Kokh, N.G. Kononova, P.P. Fedorov, S.V. Kuznetsov, Crystal growth and phase equilibria in the BaB_2O_4–NaF system, Cryst. Growth Des. 9 (2009) 4060–4063.
[6] C. Chen, Y. Wu, A. Jiang, et al., New nonlinear optical crystal LiB_3O_5, J. Opt. Soc. Am. B 6 (1989) 616–621.
[7] Y. Wu, T. Sasaki, S. Nakai, A. Yokotani, H. Tang, C. Chen, CsB_3O_5: a new nonlinear optical crystal, Appl. Phys. Lett. 62 (1993) 2614–2615.
[8] T. Sasaki, Y. Mori, M. Yoshimura, Progress in the growth of a $CsLiB_6O_{10}$ crystal and its application to ultraviolet light generation, Opt. Mater. 23 (2003) 343–351.
[9] N.G. Kononova, A.E. Kokh, P.P. Fedorov, M.A. Ferapontova, R.M. Zakalyukin, E.A. Tkachenko, Nanoporous crystalline material $LiCsB_6O_{10}$, Inorg. Mater. 38 (2002) 1264–1269.
[10] C.T. Chen, G.L. Wang, J.Y. Wang, Z.Y. Hu, Deep-UV nonlinear optical crystal $KBe_2BO_3F_2$: discovery, growth, optical properties and applications, Appl. Phys. B 97 (2009) 9–25.
[11] C.T. Chen, S.Y. Luo, X.Y. Wang, et al., A novel deep-UV nonlinear optical crystal: $RbBe_2BO_3F_2$, J. Opt. Soc. Am. B 26 (2009) 1519–1525.
[12] C. Chen, Y. Wang, B. Wu, K. Wu, W.L. Zeng, L.H. Yu, Design and synthesis of an ultraviolet-transparent nonlinear optical crystal $Sr_2Be_2B_2O_7$, Nature 373 (1995) 322–323.
[13] Z.G. Hu, Y. Mori, T. Higashiyama, et al., $K_2Al_2B_2O_7$–a new nonlinear optical borate crystal, Proc. SPIE 3556 (1998) 156–161.
[14] N. Ye, W.L. Zeng, B.C. Wu, C.T. Chen, Two new nonlinear optical crystals: $BaAl_2B_2O_7$ and $K_2Al_2B_2O_7$, Proc. SPIE 3556 (1998) 21–23.
[15] H. Hellwig, J. Liebertz, L. Bohaty, Exceptional large nonlinear optical coefficients in the monoclinic bismuth borate BiB_3O_6 (BIBO), Solid State Commun. 109 (1999) 249–251.
[16] A.V. Evorysheva, V.M. Skorikov, Efficient nonlinear optical material BiB_3O_6 (BIBO), Inorg. Mater. 45 (2009) 1461–1476.
[17] H. Wu, H. Yu, Z. Yang, X. Hou, X. Su, S. Pan, K.R. Poeppelmeier, J.M. Rondinelli, Designing a deep-ultraviolet nonlinear optical material with a large second harmonic generation response, J. Am. Chem. Soc. 135 (2013) 4215–4218, doi: http://dx.doi.org/10.1021/ja400500m.
[18] G. Aka, A. Kahn-Harari, D. Vivien, et al., A new nonlinear and neodymium laser self-frequency doubling crystal with congruent melting: $Ca_4GdO(BO_3)_3$ (GdCOB), Eur. J. Solid State Inorg. Chem. 33 (1996) 727–736.
[19] T. Iwai, M. Kobayashi, H. Furuya, et al., Crystal growth and optical characterization of rare-earth (Re) calcium oxyborate $ReCa_4O(BO_3)_3$ (Re = Y or Gd) as new nonlinear optical material, Jpn. J. Appl. Phys. 36 (1997) L276–L279.
[20] Z.G. Hu, M. Yoshimura, K. Muramatsu, et al., A new nonlinear optical crystal—$BaAlBO_3F_2$ (BABF), Jpn. J. Appl. Phys. 41 (2002) L1131–L1133.
[21] G. Wang, J. Lu, D. Cui, et al., Efficient second harmonic generation in a new nonlinear $La_2CaB_{10}O_{19}$ crystal, Opt. Commun. 209 (2002) 481–484.
[22] N. Ye, J. Stone-Sundberg, M.A. Hruschka, G. Aka, W. Kong, D.A. Keszler, Nonlinear optical crystal $Y_xLa_ySc_2(BO_3)_4$ ($x+y+z=4$), Chem. Mater. 17 (2005) 2687–2692.
[23] A.E. Kokh, N.G. Kononova, M.V. Fedorova, P.P. Fedorov, M.N. Mayakova, New nonlinear optical crystals of the $M_{1-x}Sc_{3-y}Y_{x+y}(BO_3)_4$ (M = Ce, Pr, or Nd) family, Dokl. Phys. 57 (2012) 148–150.
[24] S.V. Rashchenko, T.B. Bekker, V.V. Bakakin, et al., A new mechanism of anionic substitution in fluoride borates, J. Appl. Crystallogr. 46 (2013) 1081–1084.
[25] B.S.R. Sasrtry, F.A. Hummel, Studied in lithium oxide systems: $Li_2O{\cdot}B_2O_3$–B_2O_3, J. Am. Ceram. Soc. 41 (1958) 7.
[26] Q. Huang, J. Liang, Studies on flux systems for the single crystal growth of β-BaB_2O_4, J. Cryst. Growth 97 (1989) 720–724.
[27] V. Nikolov, P. Peshev, On the growth of β-BaB_2O_4 from high-temperature solutions: I. study of solvents of the BaO–Na_2O–B_2O_3 system, J. Solid State Chem. 96 (1992) 48–52.
[28] P.P. Fedorov, A.E. Kokh, N.G. Kononova, T.B. Bekker, Investigation of phase equilibria and growth of BBO (β-BaB_2O_4) crystals in BaO–B_2O_3–Na_2O ternary system, J. Cryst. Growth 310 (2008) 1943–1949.
[29] A.E. Kokh, N.G. Kononova, T.B. Bekker, P.P. Fedorov, E.A. Nigmatulina, A.G. Ivanova, An investigation of the growth of beta-BaB_2O_4 crystals in the BaB_2O_4–NaF system and new fluoroborate $Ba_2Na_3[B_3O_6]_2F$, Crystallogr. Rep. 54 (2009) 146–151.

[30] T.B. Bekker, P.P. Fedorov, A.E. Kokh, The ternary reciprocal system Na, Ba//BO_2, F, Cryst. Growth Des. 12 (2012) 129–134.
[31] Hongwei Yu, Shilie Pan, Hongping Wu, et al., A new congruent-melting oxyborate, $Pb_4O(BO_3)_2$ with optimally aligned BO_3 triangles adopting layered-type arrangement, J. Mater. Chem. 22 (2012) 2105–2110.
[32] Z. Yang, S. Pan, H. Yu, M.-H. Lee, Electronic structure and optical properties of the nonlinear optical crystal $Pb_4O(BO_3)_2$ by first-principles calculations, J. Solid State Chem. 198 (2013) 77–80.
[33] R.F. Geller, E.N. Bunting, The system PbO–B_2O_3, J. Res. Nat. Bur. Stand. 18 (1937) 585 RP995.
[34] V.T. Mal'tsev, A.G. Bergman, P.M. Chobanyan, V.L. Volkov, The system PbO–B_2O_3–WO_3, Russ. J. Inorg. Chem. 18 (1973) 1764–1766.
[35] H.F. McMurdie, X-ray studies of compounds in the systems PbO–B_2O_3 and K_2O–PbO–SiO_2, J. Res. Nat. Bur. Stand. 26 (1941) 489 RP1392.
[36] B. Chalmers, Principles of Solidification, R.E. Krieger Pub. Co. Huntington, New York, 1977.
[37] J.P. Hirth, G.M. Pound, Condensation and Evaporation, Macmillan, New York, 1963.
[38] P.P. Fedorov, B.P. Sobolev, L.V. Medvedeva, V.M. Reiterov, Revised phase diagrams of LiF–RF_3 (R = La–Lu, Y) systems, in: E.I. Givargizov, A.M. Melnicova (Eds.), Growth of Crystals, vol. 21, Consultants Bureau, N.Y.- London, 2002 pp. 141–154.
[39] P.P. Fedorov, B.P. Sobolev, Calculation of the metastable melting temperatures of the low temperature modifications of the rare-earth trifluorides, Russian J. Phys. Chem. 62 (1988) 447–449 (in Russian).
[40] B.P. Sobolev, I.D. Ratnikova, P.P. Fedorov, B.V. Sinitsyn, G.S. Shahkalamian, Polymorphism of ErF_3 and position of third morphotrophic transition in the lanthanide trifluoride series, Mater. Res. Bull. 11 (1976) 999–1004.
[41] P.P. Fedorov, B.P. Sobolev, Morphotropic transitions in the rare-earth trifluoride series, Crystallogr. Rep. 40 (1995) 284–290.
[42] G. Heller, Gmelin Handbuch der Anorganischer Chemie, B. 28 Borverbindunger, Teil 7, Boroxide, Borsauren, Borate, Springer, Berlin e.a. 1975.
[43] H. Bauer, G. Plotscher, Uber blediborat, PbO·B_2O_3, Z. Anorg. Allg. Chem. 350 (1967) 271–280.